Electronic Journal «Technical Acoustics»
http://webcenter.ru/~eeaa/ejta/

2004, 4

Ying-Chun Chang[1], Long-Jyi Yeh, Min-Chie Chiu

Department of Mechanical Engineering, Tatung University, Taipei, Taiwan 104, R.O.C.
e-mail: ycchang@ttu.edu.tw

Optimization on constrained single-layer absorbers by simulated annealing

Received 27.02.2004, published 07.04.2004

As the thickness of sound absorber is often confined by the necessity of worker's maintenance and access in the practical engineering work, the consideration of maximal sound absorption on the sound absorber with limited thickness becomes important and essential. In this paper, by using the simulated annealing (SA), a stochastic relaxation technique based on the analogy of the physical process of annealing metal, a single-layer absorber, including (1) one layer of perforated plate; (2) one layer of acoustic fiber; (3) one layer of air space; and (4) a rigid-backing wall, is optimized under the thickness constraints. A numerical case in dealing with pure tone noise of 350 Hz was exemplified. Before optimization, a sample was tested and compared with the experimental data for accuracy check of mathematical model. Results proved that SA optimization provides a quick and efficient approach on the design of single-layer sound absorbers under fixed thickness.

Keywords: sound absorption, transfer matrix method, shape optimization, simulated annealing

1. INTRODUCTION

Many researches of sound absorber were well developed; however, the discussion of optimization on sound absorption of the absorber under the thickness constraints was rarely accomplished even though the thickness of absorber confined by the demand of maintenance and access occurred intermittently. And so, the interest to optimize sound absorption of the absorber by adjusting the shape parameters, including (1) the perforated ratio, the depth, the face density and the holes of the perforated front plate; (2) the depth of sound absorbing material and air space, at the limited thickness of sound absorber is arising in the field of acoustics.

Yeh et al. [1] developed the shape optimization of the constrained single-layer sound absorbers by the graphic sensitivity analysis. But it is still troublesome and tedious. To solve efficiently the optimal design of sound absorbers, simulated annealing (SA) by Kirkpatrick et al. [2], based on the work of Metropolis et al. [3], was applied. The matrix transfer form for sound absorption deduced in the previous work [4] was applied for the derivation of normal sound absorption coefficient. In addition, the half-experienced formula of specific normal impedance by Delany and Bazley [5] as well as by Bolt and Ingard [6, 7] were both included in the model derivation simultaneously.

This paper provides a quick and efficient method to optimize the shape of single-layer absorber by using the matrix transfer method together with the SA searching technique.

[1]Corresponding author: Ying-Chun Chang, e-mail: ycchang@ttu.edu.tw, mailing address: Department of Mechanical Engineering, Tatung University, 40 Chungshan N. Rd., 3rdSec., Taipei, Taiwan 104, R.O.C.

2. THEORETICAL BACKGROUND

For a plane wave propagating through a partitioned and uniform section with stationary medium, the relationships of acoustic pressure and particle velocity between point 1 and point 2 can be expressed in matrix form (see Appendix) as follow:

$$\begin{pmatrix} p_1 \\ u_1 \end{pmatrix} = \begin{bmatrix} \cos(kL) & jZ_{air}\sin(kL) \\ j\sin(kL)/Z_{air} & \cos(kL) \end{bmatrix} \begin{pmatrix} p_2 \\ u_2 \end{pmatrix}. \tag{1}$$

For an acoustic wave propagating within the arbitrary medium symbolized by *mm*, the general matrix form between point 1 and point 2 is then expressed as

$$\begin{pmatrix} p_1 \\ u_1 \end{pmatrix} = \begin{bmatrix} \cos(k_{mm}L) & jZ_{mm}\sin(k_{mm}L) \\ j\sin(k_{mm}L)/Z_{mm} & \cos(k_{mm}L) \end{bmatrix} \begin{pmatrix} p_2 \\ u_2 \end{pmatrix}. \tag{2}$$

The absorber's acoustic impedance on the perforated front plate is obtained from the bottom wall of the infinity of impedance [8]. The composition of single-layer perforated absorber is illustrated in Fig. 1. As derived in Eq. (2), the relation of acoustic pressure p and acoustic particle velocity u between point 0 and point 1 is expressed as the transfer matrix and shown as below.

$$\begin{bmatrix} p_1 \\ u_1 \end{bmatrix} = \begin{bmatrix} \cos(\omega L/c_o) & j\rho_o c\sin(\omega L/c_o) \\ j\sin(\omega L/c_o)/\rho_o c_o & \cos(\omega L/c_o) \end{bmatrix} \begin{bmatrix} p_o \\ u_o \end{bmatrix}, \tag{3}$$

where p_1 is the acoustic pressure at the surface of the air layer, u_1 is the acoustic particle velocity at the surface of the air layer, p_o is the acoustic pressure at the absorber's bottom, and u_o is the acoustic particle velocity at the back plate (wall).

For a structure of "partitioned rigid wall $+L$ thickness of air $+D_f$ thickness of the acoustic fiber", the relation of acoustic pressure *p* and acoustic particle velocity *u* between point 1 and point 2 is expressed as the transfer matrix:

$$\begin{bmatrix} p_2 \\ u_2 \end{bmatrix} = \begin{bmatrix} \cos(k_{fiber}D_f) & jZ_{fiber}\sin(k_{fiber}D_f) \\ j\sin(k_{fiber}D_f)/Z_{fiber} & \cos(k_{fiber}D_f) \end{bmatrix} \begin{bmatrix} p_1 \\ u_1 \end{bmatrix}. \tag{4}$$

By adopting the formula of specific normal impedance and wave number, which is derived by Delany and Bazley [5] and valid in fibrous porous materials at the flow resistivity range *R* of 10^3~$5\text{x}10^4$ (MKS rayls/m), Eq. (4) can thus be rearranged as

$$Z_2 = (R_{fiber} + jX_{fiber})\left[\frac{\sinh(k_2)\cos(k_1) - j\sin(k_1)\cosh(k_2)}{\cos(k_1)\cosh(k_2) - j\sinh(k_2)\sin(k_1)}\right], \tag{5a}$$

$$\text{where } k_1 = (\omega/c_o)[1 + 0.0978(\rho_o f/R)^{-0.700}];\ k_2 = (\omega/c_o)[-0.189(\rho_o f/R)^{-0.595}];$$
$$R_{fiber} = \rho_o c_o[1 + 0.0571(\rho_o f/R)^{-0.754})];\ X_{fiber} = \rho_o c_o[-0.087(\rho_o f/R)^{-0.732}]. \tag{5b}$$

Next, by analyzing structure of "partitioned rigid wall $+L$ thickness of air $+D_f$ thickness of acoustic fiber + *q* thickness of the perforated front plate", the normal impedance Z_3 at the surface of perforated front plate is expressed in the matrix form:

$$\begin{bmatrix} p_3 \\ u_3 \end{bmatrix} = \begin{bmatrix} \cos(k_p q) & jZ_p \sin(k_p q) \\ j\sin(k_p q)/Z_p & \cos(k_p q) \end{bmatrix} \begin{bmatrix} p_2 \\ u_2 \end{bmatrix}. \tag{6}$$

By developing Eq. (6) and adopting the formula of specific normal impedance and wave number of perforated plate derived by Bolt and Ingard [6, 7], the normal impedance Z_3 at the surface of the perforated front plate is simplified into the complex form

$$Z_3 = Z_p \frac{Z_2 + iZ_p \tan(k_p q)}{Z_p + iZ_2 \tan(k_p q)}, \tag{7a}$$

where $Z_p = j\dfrac{32\pi f M_h}{\left(1+\dfrac{16M_h}{mN\pi^2 d^4}\right)\left(N\pi^2 d^4\right)}$; $M_h = \rho_o\left(\dfrac{\pi d^2 q}{4} + 2\dfrac{d^3}{3}\right)$. (7b)

For normal incidence, the sound absorption coefficient [9] is

$$\alpha(D_f, L, f, R, q, d, m, p\%) = 1 - \left|\frac{Z_3 - \rho_o c}{Z_3 + \rho_o c}\right|^2. \tag{8}$$

3. MODEL CHECK

Before performing the SA optimal simulation, the accuracy check of a fundamental mathematical model on single-layer sound absorber was made by an experiment, as follows.

3.1. Experimental Setup

An experiment for measuring the normal sound absorption coefficient is designed and depicted in Fig. 2. As indicated in Fig. 2, the acoustic impedance tube has been used by emitting the normal incident plane wave and by detecting the standing-wave with a movable microphone. Therefore, on the plane wave bases, the measurement is valid only when the frequency performed is under the cutoff frequency, f_c.

According to Rayleigh [10], the cutoff frequency for circular pipe is derived as $0.586 c_o / d$ where c_o is the sound speed and d is the diameter of acoustic impedance tube respectively.

3.2. Sound Absorption Coefficient

A sample of a single-layer sound absorber was simulated and tested by experiment. The accuracy comparisons between theoretical and experiment for the model were made and illustrated in Fig. 3, accordingly. As shown in Fig. 3, the result conveys that they are in good agreement. Therefore, the proposed fundamental mathematical model is acceptable. Thereafter, the developed model of single-layer sound absorber linked with SA optimization method on the constrained sound absorption system is applied in the following sections.

4. SIMULATED ANNEALING

Simulated annealing (SA) algorithm imitates the cooling process of material in a heat bath. In the physical system, annealing is the process of heating a solid to its melting phase, followed by a cooling operation until the material has crystallized. The slow cooling (annealing) allows the lowest energy state (i.e. minimum) to be reached; however, the fast cooling rate (quenching) will result in higher energy condition with the large internal energy stored inside the imperfect lattice. The basic concept behind SA was first introduced by Metropolis et al. [3]. and developed by Kirkpatrick et al. [2]. The purpose of using SA algorithm is to avoid the local optimal solution during the optimization.

The algorithm starts by generating a random initial solution and by initializing both the initial temperature (T_o) and the frozen temperature (T_{final}). The scheme of SA is a variation of the hill-climbing algorithm. All down hill movements for improvements are accepted for the decrement of the system energy. Simultaneously, SA also allows moves resulting in worse-quality solutions (uphill moves) than the current solution in order to escape from local optimum. At higher temperature, the uphill move is already in a good change. However, the change of going up hill is decreased when the temperature gets lower.

To simulate the evolution of the SA algorithm, a new random solution is chosen from the neighborhood of the current solution. If the change in energy (or objection function) is negative, the new solution is accepted to be the new current solution. Otherwise, the transition property ($p_b(T)$) of accepting the increase is computed by evaluating the Boltzmann's factor ($p_b(T)=\exp(\Delta F / CT)$) where ΔF, C and T are the difference of object function, Boltzmann constant and current temperature respectively. If the probability is greater than a random number in the interval of [0,1], the new solution is then accepted. If not, it is rejected. The algorithm iterates by perturbing the current solution and measuring the change in objection function.

Each successful replacement of the new current solution leads the decrement of new current temperature by multiplying current temperature by the cooling rate (*kk*), which is normally within 0.95 to 0.98. The process is repeated until the frozen temperature (T_{final}) is reached or until there are no changes in the objection function.

The flow diagram regarding SA optimization is described and shown in Fig. 4. As indicated in Fig. 4, to maximize the sound's absorbing coefficient, the objection function in SA is represented by the negative value ($-\alpha$) in SA optimization.

5. CASE STUDY

The noise control of a machine fan room was exemplified. Because of the periodic disturbance of the in-flow acting on the fan, the phenomenon of siren effect occurred. A pure tone of 350 Hz was identified by the formula of $f=N_b \cdot n$ where N_b and n are the number and rotational speed of blades, respectively.

For the necessity of maintenance and access, the thickness of absorber was limited to be 0.2 m. A sound absorbing material of rockwool with density 80 kg/m^3 was chosen. According to Wang's experiment [11], the flow resistance of above rockwool is about 22000 rayls/m.

For the purpose of lightness on sound absorber, the thickness (q) and face density (m) of the perforated front plate are pre-selected as q=0.0006 m; m=2.0 kg/m^2. A series of constrained conditions in the design are specified as $5.0\% \le p\% \le 50.0\%$; 0.003 m$\le d \le$0.015 m; 0.01 m$\le D_f \le$0.184 m; f=350 Hz; D_o=0.3 m; R=22000 rayls/m.

6. RESULTS AND DISCUSSION

In this case, both the initial temperature (T_o) and lower frozen temperature (T_{final}) were set as 120 and 0.00001 respectively. According to Cave et al. [12], the cooling rate (kk) was chosen as 0.95 firstly. To achieve a better approach in SA, four kinds of initial temperature were tested. In addition, the cooling rate was varied from 0.95 to 0.98 gradually.

The comparison of results for the seven sets of SA's control parameters is illustrated in Table 1. It shows that in the 1st case, the initial temperature (T_o) and the cooling rate (kk) were taken as 120 and 0.95 respectively. It has an optimal value of 0.886 in sound absorption coefficient compared to other cases.

The profiles of sound absorption curves with respect to spectrum in various initial temperature (T_o) are plotted together in Fig. 5. In addition, the profiles of sound absorption curves with respect to spectrum in various cooling rate (kk) are plotted together in Figure 6. As indicated in Figures 5 and 6, each of the sound absorption at the desired frequency of 350 Hz was very close even though the deviations of profiles existed between them.

As indicated in Table 1, the iteration will increase at the higher value of cooling rate (i.e. the slower annealing) at the same initial temperature (T_o). Otherwise, the iteration will decrease at the lower cooling rate (kk). However, the deviation of iteration time with respect to different initial temperature (T_o) at the same cooling rate (kk) is not obvious.

7. CONCLUSIONS

It has been shown that SA can be used in the optimization of sound absorber by adjusting the shape's parameters, including (1) the perforated ratio, the depth, the face density and the holes of the perforated front plate; (2) the depth of sound absorbing material and air space, at the fixed thickness of sound absorber.

SA becomes easier to be used comparing to traditional gradient methods in which both the complicated calculation in mathematic derivation and the selection of good starting point are required during optimal process [1]. The case study indicates that the SA operators of initial temperature (T_o), cooling rate (kk) and the frozen temperature (T_{final}) play essentially. The iteration in SA highly depends on the value of cooling rate. In addition, by the exemplification of pure tone's elimination, the expected sound absorption at the desired frequency of 350 Hz is well-optimized as 0.886. Consequently, the SA optimization can provide a quick and efficient approach on the design of single-layer absorbers under thickness constraints.

REFERENCES

[1] L. J. Yeh, M. C. Chiu, G. J. Lai. Computer aided design on single-layer perforated absorbers under space constraints. Proceedings of the 19-th National Conference on the Chinese Society of Mechanical Engineers. 2002, pp. 635–643.
[2] S. Kirkpatrick, C. D. Jr. Gelatt, M. P. Vecchi. Optimization by simulated annealing. Science, 1983, vol. 220, N°4598, pp. 671–680.
[3] A. Metropolis, W. Rosenbluth, M. N. Rosenbluth, H. Teller, E. Teller. Equation of static calculations by fast computing machines. The Journal of Chemical Physics, 1953, vol. 21, N°6, pp. 1087–1092.
[4] M. C. Chiu. Compact acoustic board for low frequencies: experimental study and theoretical analysis. The 180-th National Conference on C.S.M.E. 2001, C3, pp. 719–724.
[5] M. E. Delany and E. N. Bazley. Acoustical properties of fibrous absorbent materials. Applied Acoustics, 1969, 13, pp. 105–116.
[6] K. U. Ingard and R. H. Bolt. Absorption characteristics of acoustic material with perforated facings. Journal of the Acoustical Society of America, 1951, 23, pp. 533–540.
[7] R. H. Bolt. On the design of perforated facings for acoustic materials. Journal of the Acoustical Society of America, 1947, 19, pp. 917–921.
[8] D. A. Bies and C. H. Hansen. Engineering Noise Control. Unwin Hyman, 1988.
[9] Jinkyo Lee, W. Swenson, Jr. George. Compact sound absorbers for low frequencies. Noise Control Engineering Journal, 1992, 38(3), pp. 109–117.
[10] Rayleigh, Lord. The Theory of Sound, Macmillan. London, 1896.
[11] C. N. Wang and J. H. Torng. Experimental study of the absorption characteristics of some porous fibrous materials. Applied Acoustics, 2001, 62, pp. 447–459.
[12] Alex Cave, Saeid Nahavandi, Abbas Kouzani. Simulation optimization for process scheduling through simulated annealing. Proceedings of the 2002 Winter Simulation Conference, pp. 1909–1913.

APPENDIX

For three dimensional wave with moving medium, three kinds of governing equations are:
I. Mass continuity equation:

$$\rho_o \nabla \cdot \vec{u} + \frac{D\rho}{Dt} = 0 . \tag{A1}$$

II. Momentum equation:

$$\rho_o \frac{D\vec{u}}{Dt} + \nabla p = 0 . \tag{A2}$$

III. Energy equation (isentropic):

$$\left(\frac{\partial p}{\partial \rho}\right)_s = \frac{\gamma(p_o + p)}{\rho_o + \rho} \approx \frac{\gamma p_o}{\rho_o} = c_o^2 \text{ or } \frac{p}{\rho} = c_o^2 . \tag{A3}$$

By partial derivation and substitution in Eqs. (A1), (A2) and (A3), the wave governing equation yields

$$\left(\frac{D^2}{Dt^2} - c_o^2 \nabla^2\right) p = 0 , \tag{A4}$$

where $\frac{D}{Dt} = \frac{\partial}{\partial t} + \vec{V}_o \cdot \nabla$ is the total derivative. $\vec{V}_o$ is the mean velocity
For Cartesian coordinate system (for rectangular ducts)

$$\nabla^2 = \frac{\partial^2}{\partial x^2} + \frac{\partial^2}{\partial y^2} + \frac{\partial^2}{\partial z^2} . \tag{A5}$$

By using separation of variables method, it yields

$$p(x,y,z,t) = \sum_{m=0}^{\infty}\sum_{n=0}^{\infty} \cos\frac{m\pi x}{b} \cos\frac{n\pi y}{h}\left(C_{1,m,n} e^{-jk_{z,m,n}^{+} z} + C_{2,m,n} e^{+jk_{z,m,n}^{-} z}\right) e^{jwt} , \tag{A6}$$

$$u_z(x,y,z,t) = \frac{1}{\rho_o c_o} \sum_{m=0}^{\infty}\sum_{n=0}^{\infty} \cos\frac{m\pi x}{b} \sin\frac{n\pi y}{h}\left(\begin{array}{l} \dfrac{k_{z,m,n}^{+}}{k_o - Mk_{z,m,n}^{+}} C_{1,m,n} e^{-jk_{z,m,n}^{+} z} \\ + \dfrac{k_{z,m,n}^{-}}{k_o + Mk_{z,m,n}^{+}} C_{2,m,n} e^{+jk_{z,m,n}^{-} z} \end{array} \right) e^{jwt} . \tag{A7}$$

with the compatibility condition

$$k_{x,m}^2 + k_{y,n}^2 + k_{z,m,n}^2 = \left(k_o + Mk_{z,m,n}\right)^2 \text{ or} \tag{A8a}$$

$$k_{z,m,n}^2 = \left(k_o + Mk_{z,m,n}\right)^2 - \left(\frac{m\pi}{b}\right)^2 - \left(\frac{n\pi}{h}\right)^2 , \tag{A8b}$$

$$k_{z,m,n}^{\pm} = \frac{\mp Mk_o + \left[k_o^2 - (1-M^2)\left[\left(\frac{m\pi}{b}\right)^2 + \left(\frac{n\pi}{h}\right)^2\right]\right]^{1/2}}{1-M^2}. \quad \text{(A8c)}$$

Consequently, only the plane wave at fundamental mode of (m=0, n=0) would propagate if the frequency is small enough so that

$$f < \frac{c_o}{2h}\left(1-M^2\right)^{1/2}, \quad \text{(A9)}$$

where h is the larger value of the transverse dimensions of rectangular duct.

For one dimensional plane wave propagating perpendicularly through to a partitioned and uniform section with moving medium, the acoustic pressure is reduced to

$$p(z,t) = \left(C_1 e^{-jk_o z/(1+M)} + C_2 e^{+jk_o z/(1-M)}\right) e^{jwt}. \quad \text{(A10)}$$

The corresponding acoustic particle velocity is

$$u(z,t) = \left(\frac{C_1}{\rho_o c_o} e^{-jk_o z/(1+M)} - \frac{C_2}{\rho_o c_o} e^{+jk_o z/(1-M)}\right) e^{jwt}. \quad \text{(A11)}$$

Considering the boundary conditions of point 1 (z=0) and point 2 (z=L), it yields

$$\begin{pmatrix} p_1 \\ \rho_o c_o u_1 \end{pmatrix} = \begin{bmatrix} 1 & 1 \\ 1 & -1 \end{bmatrix} \begin{pmatrix} C_1 \\ C_2 \end{pmatrix}; \quad \text{(A12)}$$

$$\begin{pmatrix} p_2 \\ \rho_o c_o u_2 \end{pmatrix} = \begin{bmatrix} e^{-jk^+L} & e^{jk^-L} \\ e^{-jk^+L} & -e^{+jk^-L} \end{bmatrix} \begin{pmatrix} C_1 \\ C_2 \end{pmatrix}, \quad \text{(A13)}$$

where $k^+ = \frac{k_o}{1+M}$, $k^- = \frac{k_o}{1-M}$.

Combination of Eqs. (A12) and (A13) carries that

$$\begin{pmatrix} p_1 \\ u_1 \end{pmatrix} = e^{-j\frac{MkL}{1-M^2}} \begin{bmatrix} \cos\left(\frac{kL}{1-M^2}\right) & j\rho_o c_o \sin\left(\frac{kL}{1-M^2}\right) \\ j\sin\left(\frac{kL}{1-M^2}\right)/\rho_o c_o & \cos\left(\frac{kL}{1-M^2}\right) \end{bmatrix} \begin{pmatrix} p_2 \\ u_2 \end{pmatrix}. \quad \text{(A14)}$$

For a plane wave in a quiescent air, Eq. (A14) is reduced to

$$\begin{pmatrix} p_1 \\ u_1 \end{pmatrix} = \begin{bmatrix} \cos(kL) & jZ_{air}\sin(kL) \\ j\sin(kL)/Z_{air} & \cos(kL) \end{bmatrix} \begin{pmatrix} p_2 \\ u_2 \end{pmatrix}. \quad \text{(A15)}$$

Therefore, for a acoustic wave propagating normally into a arbitrary quiescent medium symbolized by "*mm*", the general matrix form between point 1 and point 2 is then expressed as

$$\begin{pmatrix} p_1 \\ u_1 \end{pmatrix} = \begin{bmatrix} \cos(k_{mm}L) & jZ_{mm}\sin(k_{mm}L) \\ j\sin(k_{mm}L)/Z_{mm} & \cos(k_{mm}L) \end{bmatrix} \begin{pmatrix} p_2 \\ u_2 \end{pmatrix}. \quad \text{(A16)}$$

NOMENCLATURE

This paper is constructed on the basis of the following notations:

c_o	sound speed (m·s^{-1})
d	diameter of perforated hole on the front plate (m)
D_o	thickness of absorber (m)
D_f	thickness of acoustic fiber (m)
f_c	cut-off frequency (Hz)
j	imaginary part (=$\sqrt{-1}$).
k	wave number of air
k_{fiber}	complex propagation constant of acoustic fiber
kk	cooling rate
k_{mm}	wave constant of arbitrary medium
k_p	complex propagation constant of perforated front plate
k_1	real part of complex k_{fiber}
k_2	image part of complex k_{fiber}
L	air depth of sound absorber (m)
m	surface density (kg·m^{-2})
N	hole's number on the perforated front plate per m^2
$p_b(T)$	transition probability
$p\%$	perforated ratio of front plate (%)
p_i	acoustic pressure at i (Pa)
q	thickness of perforated front plate (m)
R	acoustic flow resistance of acoustic fiber (*MKS* rayls·m^{-1})
R_{fiber}	real part of complex Z_{fiber}
T_i	current temperature (^{o}C)
T_{i+1}	next temperature (^{o}C)
T_o	initial temperature (^{o}C)
T_{final}	final temperature (=5·10^{-5} ^{o}C)
u_i	acoustic particle velocity at i (kg·s^{-1})
V_o	mean velocity of medium (m·s^{-1})
ω	angular frequency (rad s^{-1})
X_{fiber}	image part of complex Z_{fiber}
Z_{air}	characteristic impedance of air ($=\rho_o c_o$)
Z_{mm}	characteristic impedance of arbitrary medium
Z_i	specific normal impedance at i
Z_{fiber}	characteristic impedance of acoustic fiber
Z_p	characteristic impedance of perforated front plate
α	sound absorption coefficient of absorber
ρ_o	air density (kg·m^{-3})

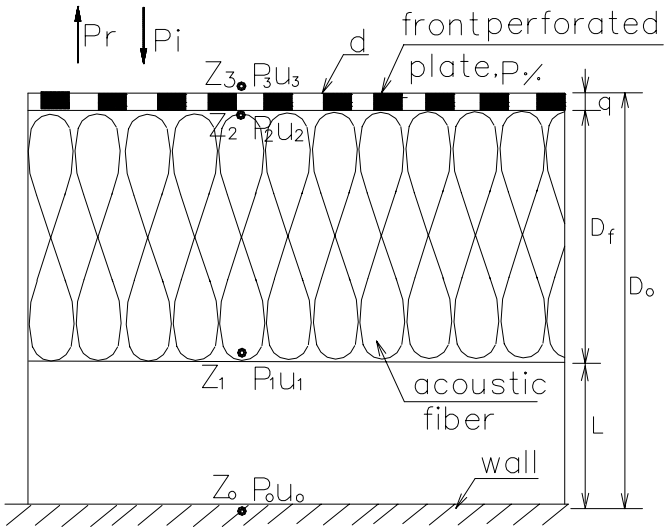

Fig. 1. Composition of a single-layer sound absorber (D_o = 0.2 m)

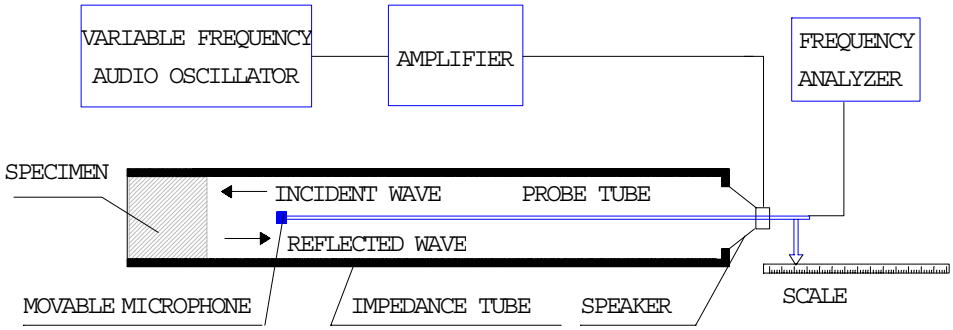

Fig. 2. Experimental setup for measurement of normal sound absorption coefficient using impedance tube

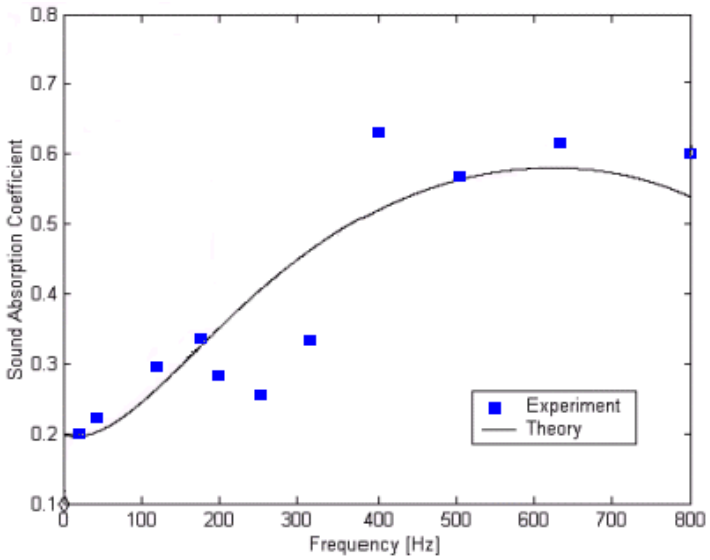

Fig. 3. Accuracy check for theoretical mode of single-layer sound absorber (L=0.05 m, D_f =0.046 m, p%=19.4%, d=0.003 m, R=8000 rayls/m, m=2 kg/m^2, q=0.001 m)

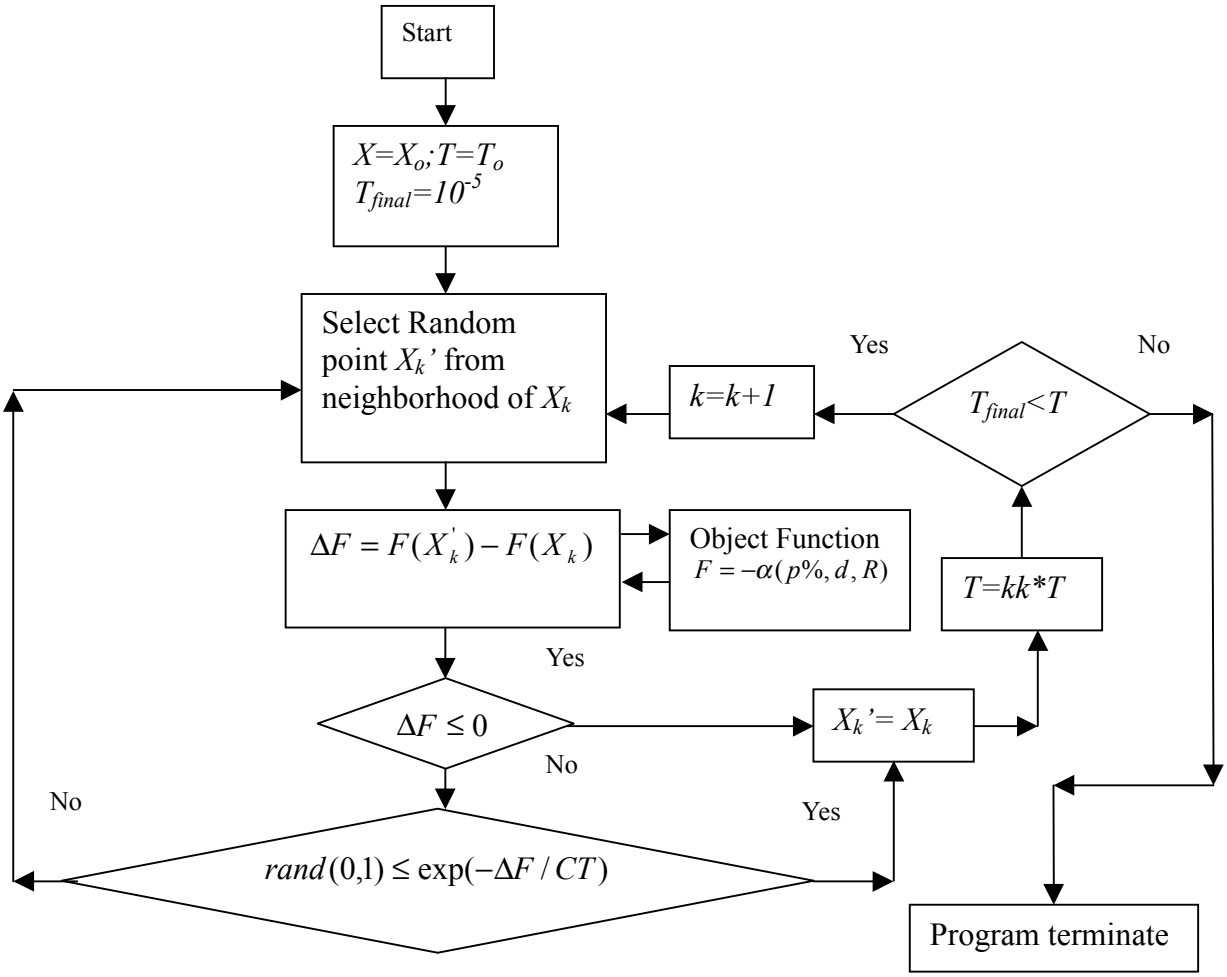

Fig. 4. A flow diagram of SA optimization

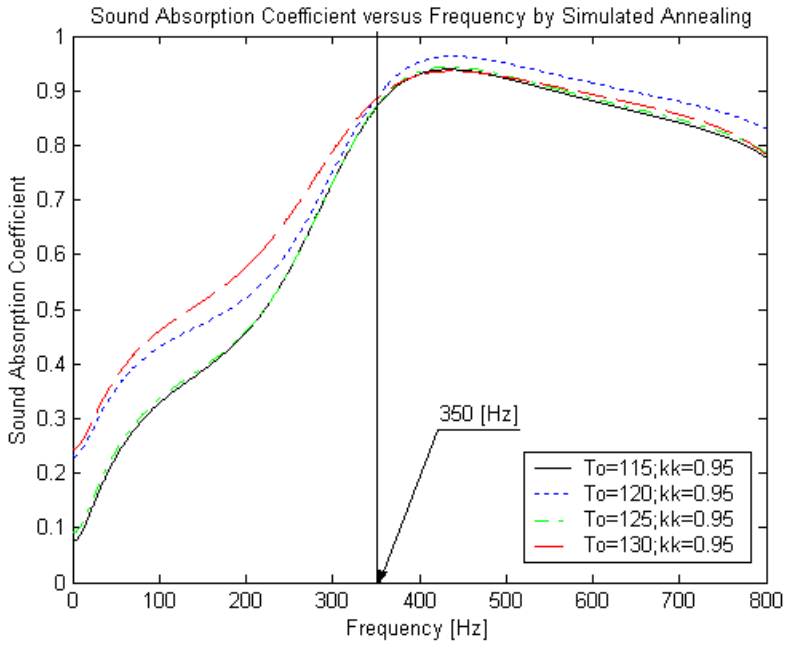

Fig. 5. Sound absorption coefficients with respect to various initial temperature (T_o)

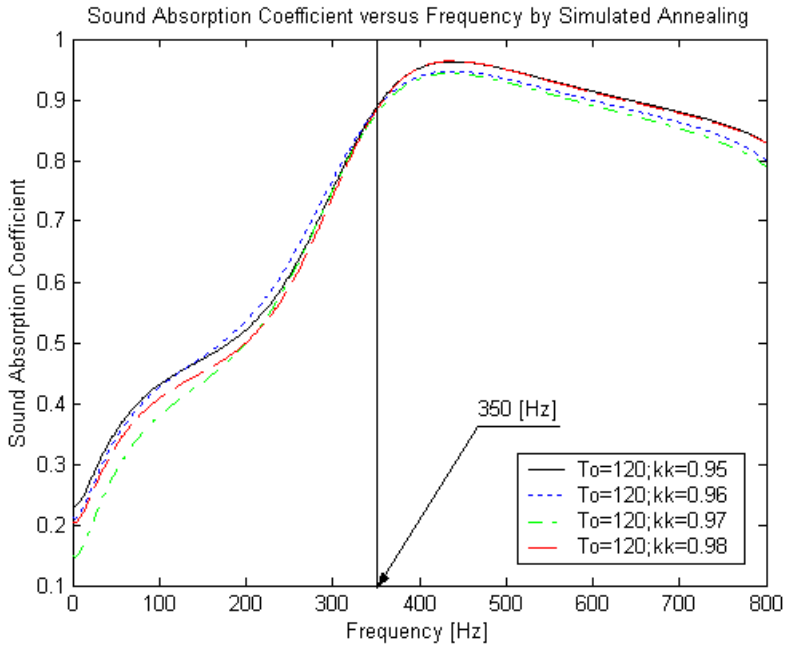

Fig. 6. Sound absorption coefficients with respect to various cooling rate (*kk*)

Table 1. Comparison of results for the variations of control parameters

	SA parameters			Results				Iterations in simulation
	T_{final}	T_o	kk	p (%)	d (m)	D_f (m)	α	
Case 1	0.00005	120	0.95	37.0	0.0033	0.1716	0.886	319
Case 2	0.00005	120	0.96	35.5	0.0035	0.1737	0.884	401
Case 3	0.00005	120	0.97	30.9	0.0047	0.1735	0.877	537
Case 4	0.00005	120	0.98	35.3	0.0037	0.1712	0.883	808
Case 5	0.00005	115	0.95	20.1	0.0063	0.1732	0.868	318
Case 6	0.00005	125	0.95	47.4	0.0130	0.1728	0.871	320
Case 7	0.00005	130	0.95	43.7	0.0037	0.1757	0.885	321